AUCTORES
Globalize your Research

International Journal of Clinical Case Reports and Reviews
Delia Teresa Sponza *

Open Access

Research Article

H2 Production from Real Wastes of Polyethylene Terephthalate and Polylactic Acid using CNx/Ni2P Nanocatalyst

Rukiye Öztekin, Delia Teresa Sponza *

Dokuz Eylül University, Engineering Faculty, Department of Environmental Engineering, Tınaztepe Campus, 35160 Buca/Izmir, Turkey.

***Corresponding Author:** Delia Teresa Sponza, Dokuz Eylül University, Engineering Faculty, Department of Environmental Engineering, Tınaztepe Campus, 35160 Buca/Izmir, Turkey.

Received Date: August 07, 2023 | **Accepted Date:** August 24, 2023 | **Published Date:** September 01, 2023

Citation: Öztekin R., Delia T. Sponza, (2023), H2 Production from Real Wastes of Polyethylene Terephthalate and Polylactic Acid using CNx/Ni2P Nanocatalyst, *International Journal of Clinical Case Reports and Reviews*, 14(4); **DOI:10.31579/2690-4861/332**

Abstract:

In this study, H_2(g) production from real wastes of polyethylene terephthalate and polylactic acid using CN_x/Ni_2P nanocatalyst was investigated with photoreforming process. Optimum experimental conditions were found at ultrasonicated 4.8 mg/ml CN_x/Ni_2P nanocatalyst, at pre-treated 20 mg/ml polyethylene terephthalate, at pre-treated 20 mg/ml polylactic acid, at 4 ml aqueous 1 M KOH, at 10 ml internal volume of sealed photoreactor under anaerobic conditions, at 1200 W Xe solar lamp, at 60 h photoreforming solar irradiation time, at AM 1.0G, at 150 mW/cm^2, at 25°C, respectively. XRD, FESEM, EDX, FTIR, TEM, DRS and XPS analyzes were performed for characterization studies of microplastics. Polyethylene terephthalate and polylactic acid measurements were measured in inductively coupled plasma mass spectrometry (ICP-MS). H_2(g) measurements were made in gas chromatography–mass spectrometry (GC-MS). The maximum 41.40 ± 5.10 and 48.60 ± 3.12 µmol H_2 / g_{sub} yields were measured for CN_x=20 mg/ml and for Ni_2P=20 mg/ml, respectively. The maximum 18.26 ± 1.18 and 52.41 ± 7.29 µmol H_2 / g_{sub} H_2(g) production yields were found for non-sonicated CN_x/Ni_2P and ultra-sonicated CN_x/Ni_2P nanocatalyst, respectively, after 24 h photoreforming solar irradition time. The maximum 123.75 ± 11.92 and 267.41 ± 24.65 µmol H_2 / g_{sub} H_2(g) production yield was measured for polyethylene terephthalate and polylactic acid, respectively, after 60 h photoreforming solar irradiation time. The maximum 6.57 ± 0.87% and 2.43 ± 0.38% stoichiometric H_2 conversion yields were observed for polyethylene terephthalate and polylactic acid, respectively, after 60 h photoreforming solar irradition time. The maximum 96 and 57 µmol H_2 / g_{sub} H_2(g) yields for polyethylene terephthalate were obtained over CN_x/Ni_2P and $^{H2N}CN_x/Ni_2P$, respectively, after 60 h photoreforming solar irradiation time. The maximum 182 and 173 µmol H_2 / g_{sub} H_2(g) yields for polylactic acid were observed over CN_x/Ni_2P and $^{H2N}CN_x/Ni_2P$, respectively, after 60 h photoreforming solar irradiation time. The maximum 4.85 ± 0.62, 88.37 ± 10.74, 26.55 ± 1.95, 21.94 ± 1.86, 75.30 ± 9.34, 60.07 ± 5.11 and 14.61 ± 2.14 µmol H_2 / g_{sub} H_2(g) production yields were obtained for Acetate, Ethylene glycol, Formate, Glycolate, Glyoxal, Lactate and Terephthalate oxidation intermediates, respectively, after 24 h photoreforming solar irradiation times. 126 nmol Acetate, 131 nmol Formate, 5 nmol Glycolate and 6200 nmol Glyoxal organic oxidation intermediates for polyethylene terephthalate with CN_x/Ni_2P nanocatalyst were found after 7 days photoreforming solar irradiation time. 67 nmol Acetate and 63 nmol Formate organic oxidation intermediates for polylactic acid with CN_x/Ni_2P nanocatalyst were obtained after 7 days photoreforming solar irradiation time. Photoreforming process is a very effective, easy to apply, economical and environmentally friendly method for the removal of plastic and microplastic wastes.

Key words: carbon nitride/nickel phosphide (CN_x/Ni_2P) nanocatalyst; hydrogen production; microplastics; photocatalysis; polyethylene terephthalate; polylactic acid

Introduction

86% of plastic packages are collected in landfills, or they are randomly mixed into the environment (Garcia et al., 2017; Geyer et al., 2017; MacArthur, 2017a; MacArthur, 2017b). Plastic pollution is not only a global environmental pollution problem; it also shows the unconscious waste of a very valuable resource that can be recycled and reused. The majority of polymers are synthesized from fossil fuels, especially petroleum derivatives (Garcia et al., 2017). It is estimated that approximately 3.5 billion barrels of oil can be saved each year if all global

plastic waste is recycled (Garcia et al., 2017). The most important problems in the widespread application of plastic recycling are; suboptimal waste management, lack of awareness and limited size of various chemicals, complexes and polymer products (MacArthur, 2017a; MacArthur, 2017b).

Pieces of polymer smaller than ≤ 5 mm are defined as microplastics; and for recycling, microplastics represent a particularly problematic group of plastics (Cozar et al., 2014; Law and Thompson, 2014; Andrady, 2015). Microplastics formed when plastic degrades over time; They are available in a wide variety of products (Law and Thompson, 2014). Very small sizes and very dilution of microplastics; making it very difficult to collect and reuse salts from the oceans (Cozar et al., 2014; Law and Thompson, 2014; Andrady, 2015), drinking water and salts (Kosuth et al., 2018; Mason et al., 2018; Pivokonsky et al., 2018) from almost all parts of the world. A disadvantage is that even the recycling of reusable plastics has some limitations. For this reason, many polymers can only be converted into lower quality products. To give an example, only 7% of recycled poly (ethylene terephthalate) (PET) bottles can be produced as re-bottles (MacArthur, 2017a). Management structures used in plastic recycling; currently far from being able to sustainably and economically treat a wide variety of plastic waste. In order to overcome these problems: in order to be able to convert the polymers at the end of use into valuable products; more functional and usable new technologies are urgently needed.

A new technology that has recently started to be used in the recovery of plastics and especially microplastics; It is a photoreformation method in which sunlight and a photocatalyst produce H_2(g) from an organic substrate and water. The basic principle in the photoreformation method is that the substrate is oxidized to other organic molecules by the excited photocatalyst, acting as an electron donor. Photogenerated electrons are transferred from the photocatalyst to a co-catalyst in the next step; they reduce water to H_2(g). H_2(g) is in very high demand in the agricultural, pharmaceutical and chemical industries, as well as in renewable energy applications; It is a very valuable raw material (DOE, 2013; IEA, 2015). One of the existing H_2(g) production technologies; In contrast to fossil fuels' steam reforming (Spath and Mann, 2001) or thermal-based approaches to converting plastic to oil (Chen et al., 2019), the key advantages of PR are; They can be run at ambient temperature and pressure, use sunlight as their sole energy input, and produce fuel cell grade H_2(g). (Wakerley et al., 2017). While the photocatalytic degradation of plastics, typically to microplastics and CO_2(g), has been investigated for years (Ohtani et al., 1992; Horikoshi et al., 1998; Tofa et al., 2019), not only plastic waste is reduced by the phtoreformation method; At the same time, a very important advantage is provided by producing valuable chemical products. The thermodynamics of the photoreformation process is also almost energy neutral (Kuehnel and Reisner, 2018): Photoreformation of ethylene glycol at 25ºC requires ΔG° = 9.2 kJ mol-1 and E°cell = -0.01 V.

Although the photoreformation of simple molecules and biomass has been investigated in detail (Puga, 2016; Pellegrin and Odobel, 2017; Kuehnel and Reisner, 2018), plastic substrates have been largely ignored. Making polymer recycling difficult; Complex structures, low water solubility and poor biodegradation also make the photoreformation method more difficult. There are only a few previous studies on the photoreformation of plastics: in one of them; While using expensive and ultraviolet (UV) absorbing TiO_2/Pt photocatalyst (Kawai and Sakata, 1981), in another; toxic CdS/CdO_x quantum dots are used (Uekert et al., 2018).

Since the polymeric carbon nitride has a composition based on CN_x, high stability, well-positioned conductivity (CB) and valence bands (VB) and the elements Carbon (C) and Nitrogen (N), which are abundant in the soil; It is of great interest as a new generation photocatalyst (Wang et al., 2009; Vilela et al., 2012; Cao et al., 2015; Gong et al., 2015). In recent years, CN_x has been proven to support solar-powered organic substrate oxidation (Su et al., 2010), pollutant degradation (Cui et al., 2012; Qiu et al., 2015), H_2(g) production (Maeda et al., 2009; Caputo et al., 2015; Lau et al., 2016), and water decomposition (Wang et al., 2009; Liu et al., 2015; Zhu et al., 2017). Photocatalytic performances; is limited to the rapid recombination of photogenerated hole-electron pairs. To overcome this limitation; Various strategies such as nonmetal doping (Zhang et al., 2010; Wang et al., 2011; Li et al., 2012), noble metal doping (Ding et al., 2011; Gao et al., 2016; Li et al., 2016) and nanoengineering of CN_x (Yang et al., 2013; Zhan et al., 2017) can be applied. As an alternative strategy, it may be aimed to design a system in which photogenerated holes or electrons are consumed faster than charge recombination reactions by accelerating charge transfer to the catalytic sites.

Carbon nitride is a non-toxic and very affordable polymeric photocatalyst (Thomas et al., 2008; Wang et al., 2009; Lin et al., 2019); With the addition of cyanamide defects, the photocatalytic efficiency can be increased (Lau et al., 2016). CN_x has visible light absorption and band edges suitable for photoreformation reactions; CB= - 0.5 V-NHE (normal ized hydrogen electrode), VB=2.2 V-NHE has a permissive band gap of 2.7 eV (Meyer et al., 2017). It is stated in the literature that CN_x is also used for photoreformation of biomass with various cocatalysts over a wide pH range (Kasap et al., 2018). With its key advantages of visible light absorption, alkalinity stability, low cost and non-toxicity, CN_x is at a level that can compete with both CdS/CdO_x and TiO_2/Pt for polymer photoreformation. Ni_2P has previously been used for H_2(g) formation with nonfunctional carbon nitride (H_2NCN_x) and a soluble sacrificial electron donor (triethanolamine) evolution (Indra et al., 2017; Ye et al., 2017; Wen et al., 2017), and has high potential for plastic PR given its alkaline compatibility and relatively high H_2(g) forming activity (Cao et al., 2017).

Kasap et al. (2016), in order to simultaneously produce aldehyde and H_2(g) from alcohol in 1/1 stoichiometry; investigated a melon type carbon nitride ($NCNCN_x$) with cyanamide surface function in combination with a molecular nickel (II) bis(diphosphine) H_2(g) evolution catalyst NiP, oxidation and proton reduction, respectively. This closed photocatalytic redox system exhibited enhanced photoactivity with $NCNCN_x$ compared to the unfunctionalized (amino-terminated) carbon nitride H_2NCN_x with superior hole quenching ability of 4-methyl benzyl alcohol (4-MBA). The slow transfer of photogenerated electrons to diffusional NiP has been observed as the overall rate-limiting step for this photocatalyst system (Kasap et al., 2016).

A noble metal-free sacrificial photocatalytic system using dysfunctional H_2NCN_x and molecular catalyst NiP was investigated (Caputo et al., 2014). When NiP is fixed in a homogeneous solution and on semiconductor surfaces (Gross et al., 2014; Leung et al., 2017; Creissen et al., 2018); It is a hydrogenase-inspired molecular H_2(g)-evolution catalyst (Helm et al., 2011; Kilgore et al., 2011) with good activity. Catalyzed by a more active and surface functionalized $NCNCN_x$ and sacrificial electron donor NiP; It is modified by a selective and almost quantitative alcohol oxidation reaction due to proton reduction (Kasap et al., 2016).

In this study, production of H_2(g) from polyethylene terephthalate and polylactic acid wastes using CN_x/Ni_2P nanocatalyst was investigated. In our experimental study, polyester microfibers and real non-recyclable plastic waste, including those contaminated with oil, were used. XRD, FESEM, EDX, FTIR, TEM, DRS and XPS analyzes were performed for characterization studies of microplastics. Polyethylene terephthalate and polylactic acid measurements were measured in inductively coupled plasma mass spectrometry (ICP-MS). H_2(g) measurements were made in gas chromatography–mass spectrometry (GC-MS).

1. Materıals and Methods

1.1. Preparation of Carbon Nitride

Nonfunctionalized carbon nitride (H_2NCN_x) was prepared by slow heating of melamine to 550°C for 3 h in a ventilated environment according to the literature procedure (Liu et al., 2015). The resulting compound was ground and powdered in a mortar. Combining cyanamide-functional CN_x, H_2NCN_x and KSCN (weight ratio=1/2); It was prepared by heating under Ar gas for 1 h at 400°C and then at 500°C for 30 min (Lau et al., 2016). After cooling the powder was washed with deionized H_2O and dried under vacuum at 60°C.

1.1. Preparation of Ni_2P

$NiCl_2.6H_2O$ and $NaH_2PO_2.H_2O$ (weight ratio=1/5) were mixed in water for 1 h and then subjected to an ultrasonic bath for 1 h; finally dried under vacuum at 60°C. The dry compound was heated at 200°C for 1 h under Ar gas with a ramp rate of 5°C/min. After cooling to 25ºC, it was washed with 2 units of black powder, 2 units of deionized H_2O and 1 unit of ethanol; It was dried under vacuum at 60°C.

1.2. Preparation of Ni_2P with Light Absorber

According to the procedure described in the literature (Indra et al., 2017), CN_x, H_2NCN_x or TiO_2 nanoparticles (NPs) (300 mg) and 20 mg $NiCl_2.6H_2O$ were taken and combined in 1 ml of deionized H_2O; It was stirred for 1 h and then sonicated for 1 h. Then, 100 mg of $NaH_2PO_2.H_2O$ was added to the mixture, mixed again and sonicated for 1 h. This mixture was dried under vacuum at 60°C and heated under Ar(g) with a rise rate of 5°C/min at 200°C for 1 h. After cooling to 25ºC, the powder mixture; washed with 3 parts of deionized H_2O and 3 parts of ethanol, respectively, and dried under vacuum at 60°C.

1.3. Pretreatment of Substrate

50 mg/l polymer was mixed at 300 rpm with our adaptation from the procedure described in the literature (Uekert et al., 2018). Then put in a closed bottle; It was immersed in 2 M aqueous semiconductor grade KOH at 40ºC for 24 h.

1.4. Generation of Photocatalytic H_2(g)

A dispersion of CN_x/Ni_2P nanocatalyst in 5 mg/ml deionized H_2O; 10 minutes were ultrasonicized with 30 second pulses at 100% amplitude followed by 5 second pauses (Kasap et al., 2018). For 0.65 ml mixture in 2 M aqueous semiconductor grade KOH; 1 ml of pretreated polymer and 0.35 ml of deionized H_2O per sample were used. Optimal experimental conditions were determined for 4 ml of 1 M KOH, 4.8 mg/ml CN_x/Ni_2P nanocatalyst, 50 mg/ml polymer, 20 mg/ml polyethylene terephthalate bottle or 15 mg/ml polyester microfibers, respectively. CN_x/Pt nanocomposites (NCs); It was made by ultrasonicating CN_x and then adding H_2PtCl_6 as a precursor, while Pt was synthesized via in situ photodeposition. Prepared samples were added to Pyrex glass photoreactor bottles with an internal volume of 10 ml and the bottles were tightly closed with rubber septa caps. After a short vortexing the samples; For 10 min GC grade analysis, it was cleaned by sparging with N_2(g) containing 2% CH_4(g) and no CH_4(g) was found in the samples after illumination without adding this internal standard. The samples were equipped with an AM 1.0 global (G) air mass filter and to remove infrared radiation; irradiated with a sunlight simulator (Newport/Oriel Sol3A Class AAA Solar Simulator, Model 94043A, 150 mW/cm^2) equipped with a water filter. Visible light experiments were performed by adding a cut-off filter for $\lambda > 400$ nm. All samples were mixed at 600 rpm and held constant at 25°C during irradiation. Considering 40 µl of reactor headspace gas for each sample; H_2(g) production in the samples was analyzed periodically by GC-MS. Excessive pressure inside the bottle; minimally observed, with an increase of 0.02 atm per 10 µmol H_2(g) produced.

1.5. Stoichiometric H_2(g) Conversion Mechanism

4 ml of 1 M KOH is taken; Samples containing 10 mg of substrate were prepared and irradiated for photocatalysis. H_2(g) conversion (%) were calculated as in **Equation 1** (Emel'yanenko et al., 2010; NIST Chemistry WebBook, 2023):

$$H_2 \text{ conversion } (\%) = 100 \text{ x } \frac{n_{H_2,exp} n^{-1}_{substrate,exp}}{n_{H_2,ideal} n^{-1}_{substrate,ideal}} \quad (1)$$

where; n_{H2}, exp: is the H_2(g) measured in experiment (mol), $n_{substrate, exp}$: is the substrate used in experiment (mol), and $n_{H2, idealn\ substrate, ideal}{}^{-1}$: is the ideal ratio of moles H_2(g) to substrate, respectively.

1.6. Calculation of Power

Power output from generated H_2(g); It was calculated according to **Equation 2:**

$$\text{Power (W)} = \frac{V_{H_2}\, n_{H_2} \rho_{H_2} u_{H_2}}{t_{irr}} \quad (2)$$

where; V_{H2}: is the molar volume of H_2(g) (24.47 l/mol at 25ºC), n_{H2}: is the moles of H_2(g) produced, ρ_{H2}: is the density of H_2(g) (8.235×10^{-5} kg/l at 25ºC), u_{H2}: is the lower heating value of H_2(g) (120×10^6 J/kg), and t_{irr}: is the irradiation time (s), respectively.

2.8. Characterization

2.8.1. X-Ray Diffraction (XRD) Analysis

Powder XRD patterns were recorded on a Shimadzu XRD-7000, Japan diffractometer using Cu Kα radiation (λ = 1.5418 Å, 40 kV, 40 mA) at a scanning speed of 1º /min in the 10-80º 2θ range. Raman spectrum was collected with a Horiba Jobin Yvon-Labram HR UV-Visible NIR (200-1600 nm) Raman microscope spectrometer, using a laser with the wavelength of 512 nm. The spectrum was collected from 10 scans at a resolution of 2 /cm. The zeta potential was measured with a SurPASS Electrokinetic Analyzer (Austria) with a clamping cell at 300 mbar.

2.8.2. Field Emission Scanning Electron Microscopy (FESEM)

The morphological features and structure of the experimental samples were determined by Field Emission Scanning Electron Microscopy (FESEM) (FESEM, Hitachi S-4700).

2.8.3. Energy Dispersive X-Ray (EDX) Spectroscopy Analysis

The elements on the surface of the experimental samples were analyzed using energy dispersive X-ray analysis (EDX) with EDX spectrometry device (TESCAN Co., Model III MIRA).

2.8.4. Fourier Transform Infrared Spectroscopy (FTIR) Analysis

The FTIR spectra of experimental samples were recorded using the FT-NIR spectroscope (RAYLEIGH, WQF-510).

2.8.5. *Transmission Electron Microscopy* (TEM) Analysis

The obtained experimental samples were collected and harvested by centrifugation (8000 rpm, 5 min), washed twice with deionized H_2O, and resuspended in ethanol (C_2H_6O) and dripped onto a carbon-coated copper (Cu) *Transmission Electron Microscopy* (TEM) grid. Vacuum drying then occurred to the experimental samples for 24 h at 25ºC room temperature. The dry samples on the Cu grid were viewed and examined by TEM Analysis recorded in a JEOL JEM 2100F, Japan under 200 kV accelerating voltage. The size and structure of the experimental samples were identified with TEM analysis.

2.8.6. Diffuse Reflectance UV-Vis Spectra (DRS) Analysis

DRS Analysis in the range of 200–800 nm was recorded on a Cary 5000 UV-Vis Spectrophotometer from Varian. DRS was used to monitor the experimental samples.

2.8.7. X-Ray Photoelectron Spectroscopy (XPS) Analysis

The valence state of the experimental samples were investigated and was analyzed using XPS (ESCALAB 250Xi, England). XPS used an Al Kα source and surface chemical composition and reduction state analyses was done, with the core levels recorded using a pass energy of 30 eV (resolution approximately 0.10 eV). The peak fitting of the individual core-levels was done using XPS-peak 41 software, achieving better fitting and component identification. All binding energies were calibrated to the C 1s peak originating from C–H or C–C groups at 284.6 eV

2.8.8. Inductively Coupled Plasma Mass Spectrometry (ICP-MS) Analysis

The Agilent 8800 ICP-MS instrument (Agilent Technologies, Japan) was used to determine different concentrations of polyethylene terephthalate and polylactic acid. For analysis, the samples were acid digested in closed Savillex® PFA beakers prior to ICP-MS. 5 ml of suspended sample in PBS was centrifuged at 10000 ×g for 30 min, after which the supernatant was removed. The resulting pellet was acid digested with 1.5 ml of 14 mol/l HNO_3 and 0.5 ml of 9.8 mol/l H_2O_2. The closed beakers were heated to 115°C overnight on a hot plate. After complete mineralization, the digestates were evaporated at 90°C until dryness, then redissolved in 2.0 ml of 0.35 mol/l HNO_3. This solution was further diluted with 0.35 mol/l HNO_3 and rhodium (Rh) was added as the internal standard (final concentration = 2 µg/l) to compensate for potential matrix effects and/or signal instability.

2.8.9. Gas Chromatography–Mass Spectrometry (*GC-MS*)

Gas chromatography–mass spectrometry (*GC-MS*) and gas chromatograph (GC) (Agilent Technology model 6890N) equipped with a mass selective detector (Agilent 5973 inert MSD). Mass spectra were recorded using a VGTS 250 spectrometer equipped with a capillary SE 52 column (HP5-MS 30 m, 0.25 mm ID, 0.25 µm) at 220°C with an isothermal program for 10 min. The initial oven temperature was kept at 50ºC for 1 min, then raised to 220ºC at 25ºC/min and from 200 to 300ºC at 8ºC/min, and was then maintained for 5.5 min. High purity He (g) was used as the carrier gas at constant flow mode (1.5 ml/min, 45 cm/s linear velocity). All H_2(g) measurements of the experimental samples were made in the GC-MS device.

2. Results and Discussions

2.1. Characterizations

2.1.1. XRD Analysis

The results of XRD analysis were observed after H2(g) production from real wastes of polyethylene terephthalate and polylactic acid using CNx/Ni2P nanocatalyst with photoreforming process (Figure 1). The characterization peaks were found at 2θ values of 7.74o, 46.10o, 28.16o, 36.11o and 43.87o, respectively, and which can also be indexed as (101), (210), (204), (312) and (222), respectively (Figure 1).

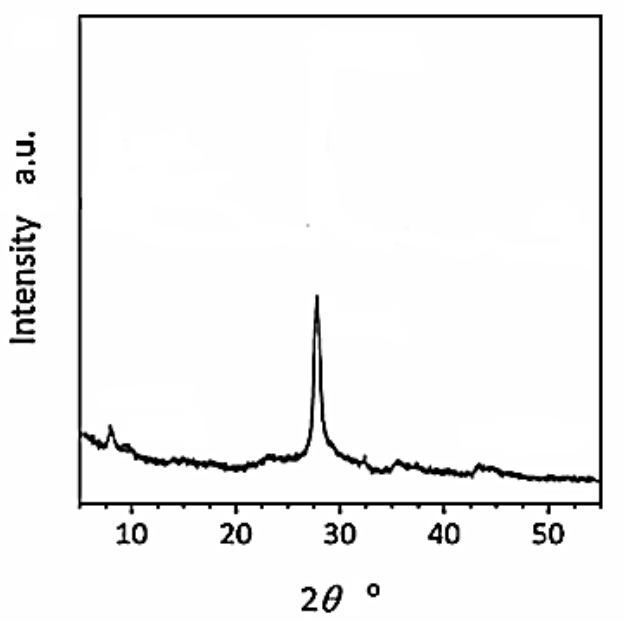

Figure 1: XRD spectra of CN_x/Ni_2P nanocatalyst after photoreforming process for H_2(g) production from real wastes of polyethylene terephthalate and polylactic acid.

1.1.1. FESEM Analysis

The morphological features of CN_x/Ni_2P nanocatalyst was characterized through FESEM images before photoreforming process (**Figure 2a**) and after photoreforming process (**Figure 2b**), respectively.

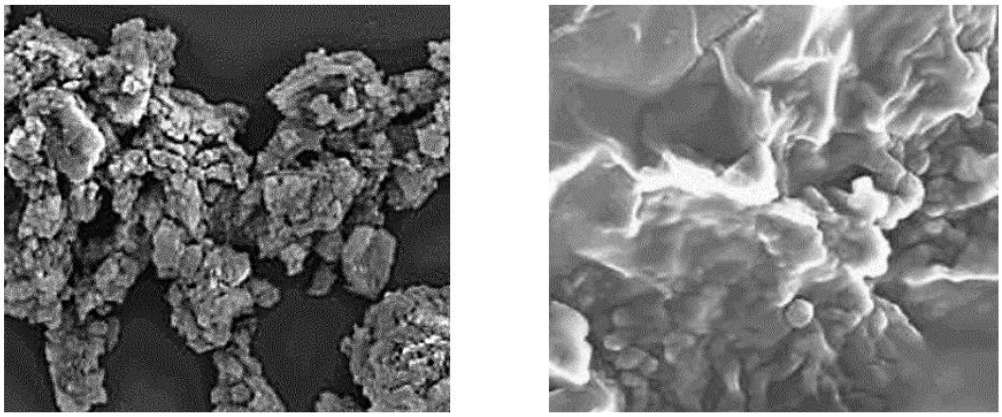

Figure 2: FESEM images of CN_x/Ni_2P nanocatalyst **(a)** before photoreforming process (**b)** after photoreforming process for $H_2(g)$ production from real wastes of polyethylene terephthalate and polylactic acid (FESEM size: 4 μm).

1.1.2. EDX Analysis

The results of EDX analysis were found after $H_2(g)$ production from real wastes of polyethylene terephthalate and polylactic acid using CN_x/Ni_2P nanocatalyst with photoreforming process (**Figure 3**).

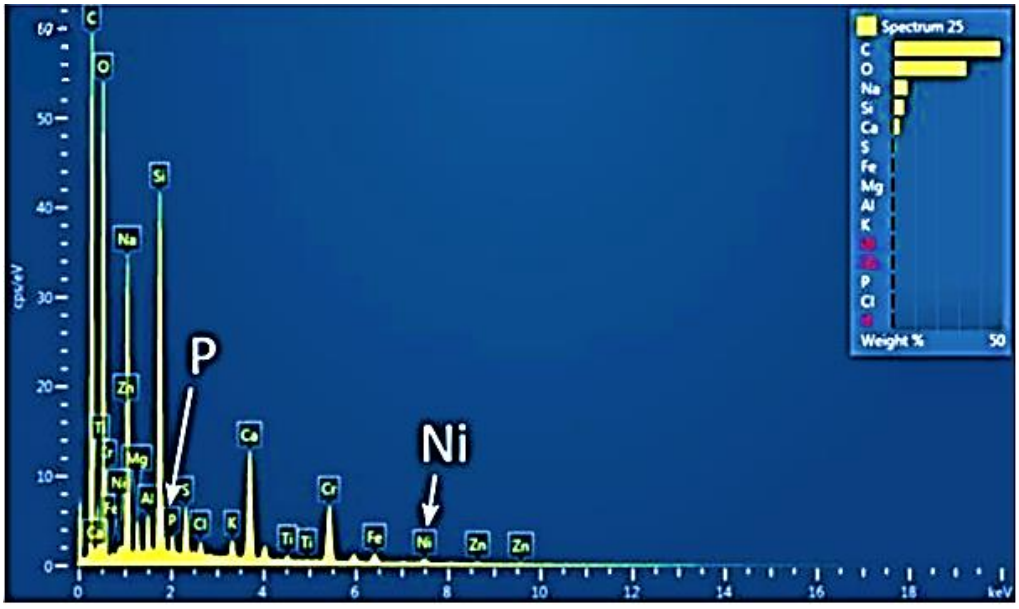

Figure 3: EDX spectrum of CN_x/Ni_2P nanocatalyst after photoreforming process for $H_2(g)$ production from real wastes of polyethylene terephthalate and polylactic acid.

1.1.3. FTIR Analysis

The FTIR spectrum of CN_x/Ni_2P nanocatalyst was measured to $H_2(g)$ production from real wastes of polyethylene terephthalate and polylactic acid after photoreforming process (**Figure 4**). The main peaks of FTIR spectrum for CN_x/Ni_2P nanocatalyst was observed at 3700 1/cm, 2250 1/cm, 2010 1/cm, 1870 1/cm, 1600 1/cm, 1150 1/cm, 960 1/cm and 830 1/cm wavenumber, respectively (**Figure 4**).

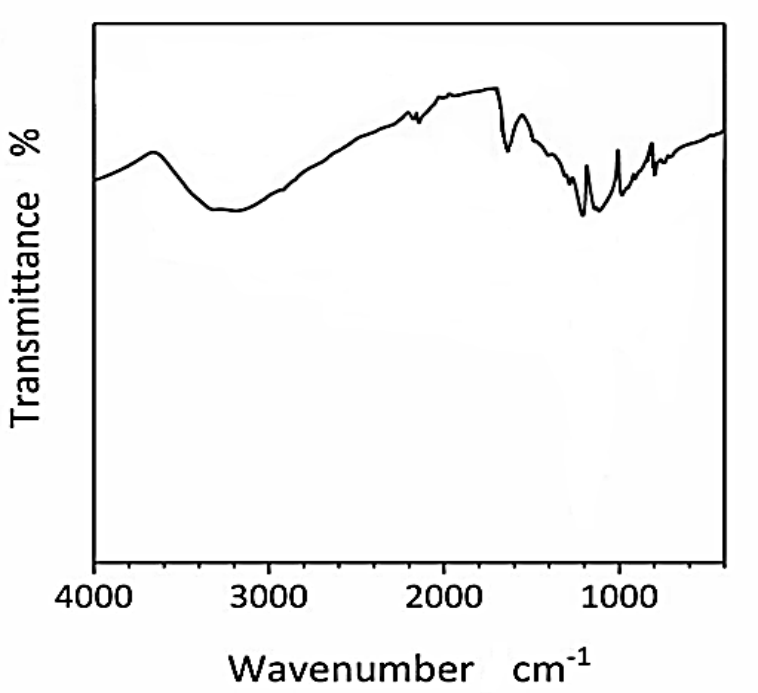

Figure 4: FTIR spectrum of CN_x/Ni_2P nanocatalyst after photoreforming process for $H_2(g)$ production from real wastes of polyethylene terephthalate and polylactic acid.

1.1.4. TEM Analysis

The TEM images of CN_x/Ni_2P nanocatalyst was obtained to $H_2(g)$ production from real wastes of polyethylene terephthalate and polylactic acid after photoreforming process (**Figure 5**).

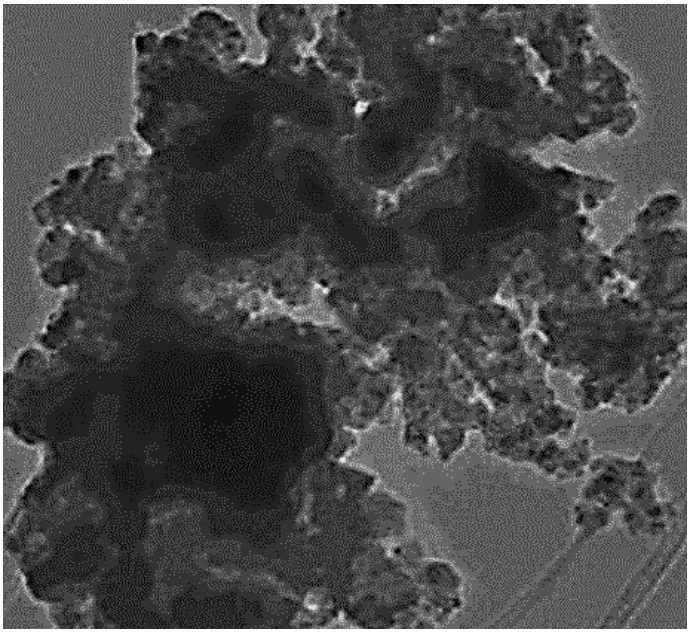

Figure 5: TEM images of CN_x/Ni_2P nanocatalyst after photoreforming process for $H_2(g)$ production from real wastes of polyethylene terephthalate and polylactic acid.

1.1.5. DRS Analysis

The DRS spectrum of CN_x/Ni_2P nanocatalyst was observed to $H_2(g)$ production from real wastes of polyethylene terephthalate and polylactic acid after photoreforming process (**Figure 6**). The DRS spectra of CN_x/Ni_2P nanocatalyst was recorded in the wavelength range from 300 nm to 600 nm using diffuse reflectance UV-V is spectra (**Figure 6**). The DRS spectrum absorption peaks of CN_x/Ni_2P nanocatalyst were found at wavelengths of 310 nm, 320 nm, 335 nm, 348 nm and 425 nm, respectively, for CN_x/Ni_2P nanocatalyst after photoreforming process (**Figure 6**).

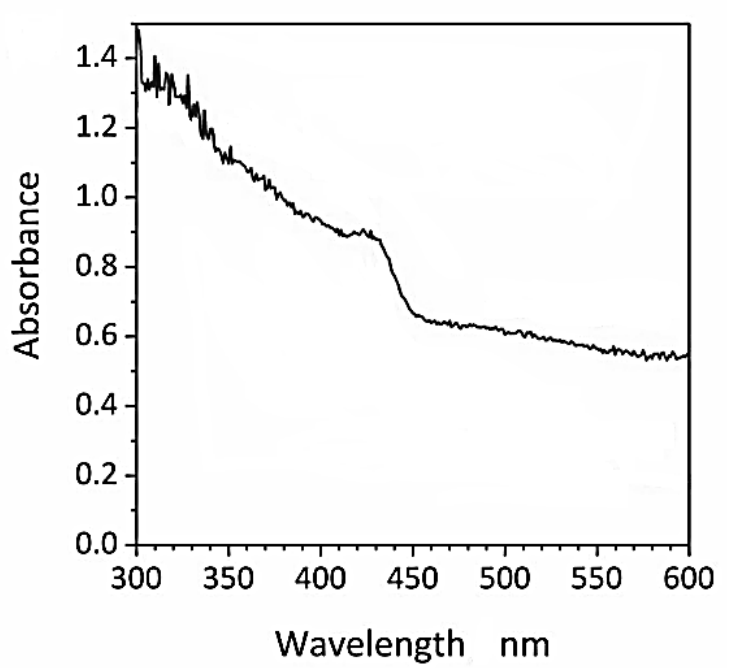

Figure 6: The DRS spectrum of CN_x/Ni_2P nanocatalyst after photoreforming process for H_2(g) production from real wastes of polyethylene terephthalate and polylactic acid.

1.1.6. XPS Analysis

The XPS analysis of CN_x/Ni_2P nanocatalyst was found to H_2(g) production from real wastes of polyethylene terephthalate and polylactic acid after photoreforming process (**Figure 7**). The results of XPS analysis were measured for N_{1s} edge of CN_x/Ni_2P nanocatalyst (**Figure 7a**) and P_{2p} edge of CN_x/Ni_2P nanocatalyst (**Figure 7b**), respectively. The binding energy value for N_{1s} edge of CN_x/Ni_2P nanocatalyst was measured to 398.76 eV for N=C bond and 400.95 eV for N-C bond, respectively (**Figure 7a**). The binding energy value for P_{2p} edge of CN_x/Ni_2P nanocatalyst was observed to 133.11 eV for PO_x (**Figure 7b**).

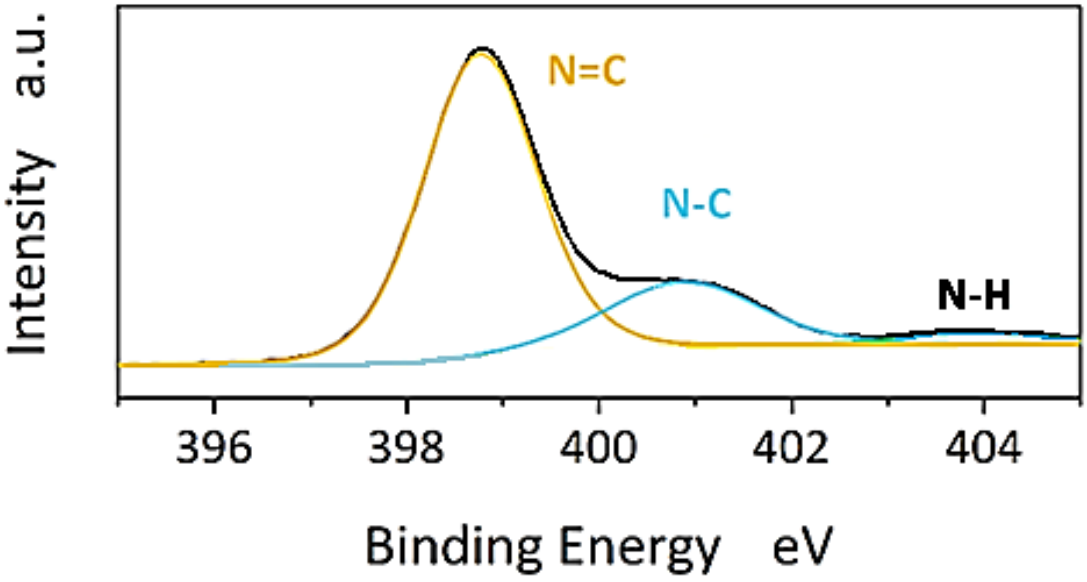

(a)

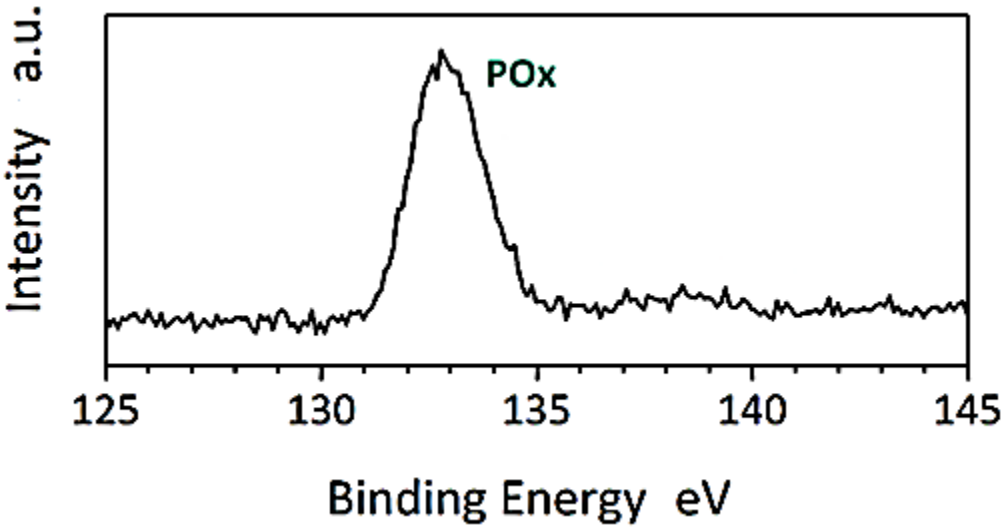

(b)

Figure 7: XPS spectra of **(a)** N_{1s} edge of CN_x/Ni_2P nanocatalyst and **(b)** P_{2p} edge of CN_x/Ni_2P nanocatalyst after photoreforming process for H_2(g) production from real wastes of polyethylene terephthalate and polylactic acid.

2. Photoreforming Experiments of Polyethylene Terephthalate and Polylactic Acid for H_2(g) Production

Photoreforming conditions for H2(g) production from real wastes of polyethylene terephthalate and polylactic acid with CNxNi2P nanocatalyst was summarized at Table 1. The maximum 41.40 ± 5.10 µmol H2 / gsub yield was measured for CNx=20 mg/ml, at ultrasonicated 4.8 mg/ml CNx/Ni2P nanocatalyst, at pre-treated 20 mg/ml polyethylene terephthalate, at pre-treated 20 mg/ml polylactic acid, at 4 ml aqueous 1 M KOH, at 10 ml internal volume of sealed photoreactor under anaerobic conditions, at 1200 W Xe solar lamp, at 24 h, at AM 1.0G, at 150 mW/cm2, at 25°C, respectively (Table 1).

Parameters (Unit)	Concentrations	Activity (µmol H_2 / g_{cat} .h)	H_2(g) Yield (µmol H_2 / g_{sub})
CN_x (mg/ml))	5	2.39 ± 0.15	1.47 ± 0.45
	10	32.40 ± 4.05	2.18 ± 0.375
	20	34.65 ± 4.82	41.40 ± 5.10
	50	33.74 ± 4.52	33.15 ± 1.65
Ni_2P (mg/ml)	5	9.18 ± 2.81	3.17 ± 0.19
	10	13.68 ± 0.70	41.40 ± 5.10
	20	35.17 ± 5.4	48.60 ± 3.12
	50	30.17 ± 3.73	44.10 ± 2.25
Note: Yields and activities are cumulative values. The standard deviation (σ) calculated from 3 samples.			

Table 1: Photoreforming conditions for H2(g) production from real wastes of polyethylene terephthalate and polylactic acid with CNxNi2P nanocatalyst (Experimental conditions: at ultrasonicated 4.8 mg/ml CNx/Ni2P nanocatalyst, at pre-treated 20 mg/ml polyethylene terephthalate, at pre-treated 20 mg/ml polylactic acid, at 4 ml aqueous 1 M KOH, at 10 ml internal volume of sealed photoreactor under anaerobic conditions, at 1200 W Xe solar lamp, at 24 h, at AM 1.0G, at 150 mW/cm2, at 25°C, respectively).The maximum 48.60 ± 3.12 µmol H2 / gsub yield was measured for Ni2P=20 mg/ml, at ultrasonicated 4.8 mg/ml CNx/Ni2P nanocatalyst, at pre-treated 20 mg/ml polyethylene terephthalate, at pre-treated 20 mg/ml polylactic acid, at 4 ml aqueous 1 M KOH, at 10 ml internal volume of sealed photoreactor under anaerobic conditions, at 1200 W Xe solar lamp, at 24 h, at AM 1.0G, at 150 mW/cm2, at 25°C, respectively (Table 1).

Optimization was achieved for maximum total H2(g) production under all experimental conditions (CNx loading, Ni2P loading, CNx/Ni2P photocatalyst concentration, polyethylene terephthalate, polylactic acid, polymer concentration, photoreforming time, temperature, pH, and irradiation solar light conditions…etc.) (Table 1). Harsh conditions (e.g., high pH) are often required to solubilize plastic, and polymer photoreforming withCNx/Ni2P improves significantly with increasing pH values, from 41.40 µmol H2 / gsub, at 4 ml aqueous 1 M KOH, at 10 ml internal volume of sealed photoreactor under anaerobic conditions, at 1200 W Xe solar lamp, at 24 h, at AM 1.0G, at 150 mW/cm2, at 25°C, respectively (Table 1).

Comparison of photoreforming with non-sonicated versus ultra-sonicated CNx/Ni2P nanocatalyst was determined at Table 2. Experimental conditions were optimized at 4.8 mg/ml CNx/Ni2P, 20 mg/ml polyethylene terephthalate, pre-treated 20 mg/ml polylactic acid, 4 ml aqueous 1 M KOH, 10 ml internal volume of sealed photoreactor under anaerobic conditions, at 1200 W Xe solar lamp, at 24 h, at AM 1.0G, at 150 mW/cm2, at 25°C, respectively (Table 2).

The CNx/Ni2P nanocatalyst was ultrasonicated in H2O for 10 min according to a procedure reported in the literature (Kasap et al., 2018). This ultrasonication process is known to increase the surface area and activity of the CNx/Ni2P nanocatalyst (Kasap et al., 2018).

Parameters	Time (h)	Activity (µmol H_2 / g_{cat} .h)	H_2(g) Yield (µmol H_2 / g_{sub})
None sonication	6	22.65 ± 1.20	11.59 ± 0.57
	12	16.88 ± 0.77	13.42 ± 0.88
	18	7.43 ± 0.53	15.28 ± 1.09
	24	4.60 ± 0.37	18.26 ± 1.18
With sonication	6	29.71 ± 1.96	22.06 ± 1.09
	12	31.44 ± 3.78	24.89 ± 1.56
	18	33.57 ± 4.12	41.54 ± 5.11
	24	37.68 ± 4.94	52..41 ± 7.29
Note: Yields and activities are cumulative values. The standard deviation (σ) calculated from 3 samples.			

Table 2: Comparison of photoreforming with non-sonicated versus ultra-sonicated CN_x/Ni_2P nanocatalyst (Experimental conditions: at 4.8 mg/ml CN_x/Ni_2P, at pre-treated 20 mg/ml polyethylene terephthalate, at pre-treated 20 mg/ml polylactic acid, at 4 ml aqueous 1 M KOH, at 10 ml internal volume of sealed photoreactor under anaerobic conditions, at 1200 W Xe solar lamp, at 24 h, at AM 1.0G, at 150 mW/cm^2, at 25°C, respectively).

The maximum 18.26 ± 1.18 µmol H_2 / g_{sub} H_2(g) production yield of non-sonicated CN_x/Ni_2P nanocatalyst was observed during photoreforming process, after 24 h photoreforming solar irradition time, at 4.8 mg/ml CN_x/Ni_2P, at 20 mg/ml polyethylene terephthalate, at pre-treated 20 mg/ml polylactic acid, at 4 ml aqueous 1 M KOH, at 10 ml internal volume of sealed photoreactor under anaerobic conditions, at 1200 W Xe solar lamp, at AM 1.0G, at 150 mW/cm^2, at 25°C, respectively (**Table 2**) The maximum 52.41 ± 7.29 µmol H_2/g_{sub} H_2(g) production yield of ultra-sonicated CN_x/Ni_2P nanocatalyst was measured during photoreforming process, after 24 h photoreforming solar irradition time, at 4.8 mg/ml CN_x/Ni_2P, at 20 mg/ml polyethylene terephthalate, at pre-treated 20 mg/ml polylactic acid, at 4 ml aqueous 1 M KOH, at 10 ml internal volume of sealed photoreactor under anaerobic conditions, at 1200 W Xe solar lamp, at AM 1.0G, at 150 mW/cm^2, at 25°C, respectively (**Table 2**). The photoreforming of pre-treated polyethylene terephthalate and pre-treated polylactic acid with CN_x/Ni_2P was obtained at **Table 3.**Photoreforming experimental conditions was optimized at ultra-sonicated 4.8 mg/ml CN_x/Ni_2P, at pre-treated 50 mg/ml polymer, at 4 ml aqueous 1 M KOH, at 10 ml internal volume of sealed photoreactor under anaerobic conditions, at 1200 W Xe solar lamp, at 24 h, at AM 1.0G, at 150 mW/cm^2, at 25°C, respectively.

Parameters	Time (h)	Activity (µmol H_2 / g_{cat} .h)	H_2(g) Yield (µmol H_2 / g_{sub})
Polyethylene Terephthalate	6	35.75 ± 1.25	5.86 ± 0.29
	12	38.27 ± 1.95	9.80 ± 0.50
	18	39.70 ± 2.03	49.66 ± 4.55
	24	41.45 ± 3.15	63.16 ± 7.04
	36	44.32 ± 3.94	68.14 ± 7.39
	48	51.36 ± 5.02	72.00 ± 6.90
	54	55.24 ± 5.82	108.5 ± 11.25
	60	60.77 ± 6.39	123.75 ± 11.92
Polylactic Acid	6	64.50 ± 7.15	8.25 ± 0.41
	12	68.05 ± 7.32	14.90 ± 1.05
	18	69.96 ± 7.45	89.55 ± 9.06
	24	72.90 ± 7.78	116.74 ± 11.48
	36	75.04 ± 8.05	129.64 ± 12.36
	48	83.11 ± 9.30	234.15 ± 18.54
	54	84.70 ± 9.65	246.32 ± 22.82
	60	87.53 ± 9.92	267.41 ± 24.65
Note: Yields and activities are cumulative values. The standard deviation (σ) calculated from 3 samples.			

Table 3: Photoreforming of pre-treated polyethylene terephthalate and pre-treated polylactic acid with CN_x/Ni_2P (Experimental conditions: at ultra-sonicated 4.8 mg/ml CN_x/Ni_2P, at pre-treated 50 mg/ml polymer, at 4 ml aqueous 1 M KOH, at 10 ml internal volume of sealed photoreactor under anaerobic conditions, at 1200 W Xe solar lamp, at 24 h, at AM 1.0G, at 150 mW/cm^2, at 25°C, respectively).

The maximum 123.75 ± 11.92 µmol H_2 / g_{sub} H_2(g) production yield was measured during photoreforming process for polyethylene terephthalate after 60 h photoreforming solar irradiation time, at ultra-sonicated 4.8 mg/ml CN_x/Ni_2P, at pre-treated 50 mg/ml polymer, at 4 ml aqueous 1 M KOH, at 10 ml internal volume of sealed photoreactor under anaerobic conditions, at 1200 W Xe solar lamp, at AM 1.0G, at 150 mW/cm^2, at 25°C, respectively (**Table 3**).

The maximum 267.41 ± 24.65 µmol H_2 / g_{sub} H_2(g) production yield was recorded during photoreforming process for polylactic acid after 60 h photoreforming solar irradiation time, at ultra-sonicated 4.8 mg/ml CN_x/Ni_2P, at pre-treated 50 mg/ml polymer, at 4 ml aqueous 1 M KOH,

at 10 ml internal volume of sealed photoreactor under anaerobic conditions, at 1200 W Xe solar lamp, at AM 1.0G, at 150 mW/cm^2, at 25°C, respectively (**Table 3**). The stoichiometric H_2 conversion calculations for polyethylene terephthalate and polylactic acid were calculated at **Table 4**. The maximum 6.57 ± 0.87% stoichiometric H_2 conversion yield was measured for polyethylene terephthalate during photoreforming process after 60 h photoreforming solar irradition time, at 4.8 mg/ml CN_x/Ni_2P, at 20 mg/ml polyethylene terephthalate, at 50 mg/ml polymer, at 4 ml aqueous 1 M KOH, at 10 ml internal volume of sealed photoreactor under anaerobic conditions, at 1200 W Xe solar lamp, at AM 1.0G, at 150 mW/cm^2, at 25°C, respectively (**Table 4).**

Parameters	**N_{100}% (mol H_2 / mol_{sub})**	**Time (h)**	**N_{yield} (mol H_2 / mol_{sub})**	**Conversion (%)**
Polyethylene Terephthalate		15	0.041 ± 0.004	0.81 ± 0.09
	5.0 [a]	30	0.060 ± 0.006	1.21 ± 0.12
		45	0.182 ± 0.023	3.63 ± 0.45
		60	0.330 ± 0.044	6.57 ± 0.87
Polylactic Acid	5.0	15	0.024 ± 0.003	0.41 ± 0.05
		30	0.039 ± 0.006	0.43 ± 0.06
		45	0.092 ± 0.018	1.53 ± 0.30
		60	0.146 ± 0.023	2.43 ± 0.38
a: assumed that only the ethylene glycol component of polyethylene terephthalate is oxidized.				
Note: Yields and activities are cumulative values. The standard deviation (σ) calculated from 3 samples.				

Table 4: Stoichiometric H_2 conversion calculations (Experimental conditions: 4.8 mg/ml CN_x/Ni_2P, at pre-treated 20 mg/ml polyethylene terephthalate, at pre-treated 20 mg/ml polylactic acid, at 50 mg/ml polymer, at 4 ml aqueous 1 M KOH, at 10 ml internal volume of sealed photoreactor under anaerobic conditions, at 1200 W Xe solar lamp, at 24 h, at AM 1.0G, at 150 mW/cm^2, at 25°C, respectively).

The maximum 2.43 ± 0.38% stoichiometric H_2 conversion yield was observed for polylactic acid during photoreforming process after 60 h photoreforming solar irradition time, at 4.8 mg/ml CN_x/Ni_2P, at 20 mg/ml polylactic acid, at 50 mg/ml polymer, at 4 ml aqueous 1 M KOH, at 10 ml internal volume of sealed photoreactor under anaerobic conditions, at 1200 W Xe solar lamp, at AM 1.0G, at 150 mW/cm^2, at 25°C, respectively (**Table 4**). Values reported for CdS/CdO_x under the same conditions were 16.6 ± 1.0% for polyethylene terephthalate and 38.8 ± 4.0% for polylactic acid during photoreforming process (Uekert et al., 2018). It should also be noted that, consistent with previous reports, these calculations assume that only the aliphatic portion of the polyethylene terephthalate is oxidized during photoreforming process (Uekert et al., 2018). Comparison of photoreforming of polyethylene terephthalate and polylactic acid over CN_x/Ni_2P and $^{H2N}CN_x/Ni_2P$ were shown at **Figure 8.** 11, 19, 33, 55, 67 and 79 μmol H_2 / g_{sub} H_2(g) yields for polyethylene terephthalate over CN_x/Ni_2P were observed after 5, 10, 20, 30, 40 and 50 h photoreforming solar irradiation times, respectively, at 4.8 mg/ml CN_x/Ni_2P photocatalyst, at pre-treated 20 mg/ml polyethylene terephthalate, at 4 ml aqueous 1 M KOH, at 10 ml internal volume of sealed photoreactor under anaerobic conditions, at 1200 W Xe solar lamp, at AM 1.0G, at 150 mW/cm^2, at 25°C, respectively (**Figure 8a**). The maximum 96 μmol H_2 / g_{sub} H_2(g) yields for polyethylene terephthalate over CN_x/Ni_2P were obtained after 60 h photoreforming solar irradiation time, at 4.8 mg/ml CN_x/Ni_2P photocatalyst, at pre-treated 20 mg/ml polyethylene terephthalate, at 4 ml aqueous 1 M KOH, at 10 ml internal volume of sealed photoreactor under anaerobic conditions, at 1200 W Xe solar lamp, at AM 1.0G, at 150 mW/cm^2, at 25°C, respectively (**Figure 8a**). 5, 21, 38, 42, 44 and 49 μmol H_2 / g_{sub} H_2(g) yields for polyethylene terephthalate over $^{H2N}CN_x/Ni_2P$ were measured after 5, 10, 20, 30, 40 and 50 h photoreforming solar irradiation times, respectively, at 4.8 mg/ml CN_x/Ni_2P photocatalyst, at pre-treated 20 mg/ml polyethylene terephthalate, at 4 ml aqueous 1 M KOH, at 10 ml internal volume of sealed photoreactor under anaerobic conditions, at 1200 W Xe solar lamp, at AM 1.0G, at 150 mW/cm^2, at 25°C, respectively (**Figure 8a**). The maximum 57 μmol H_2 / g_{sub} H_2(g) yields for polyethylene terephthalate over $^{H2N}CN_x/Ni_2P$ were obtained after 60 h photoreforming solar irradiation time, at 4.8 mg/ml CN_x/Ni_2P photocatalyst, at pre-treated 20 mg/ml polyethylene terephthalate, at 4 ml aqueous 1 M KOH, at 10 ml internal volume of sealed photoreactor under anaerobic conditions, at 1200 W Xe solar lamp, at AM 1.0G, at 150 mW/cm^2, at 25°C, respectively (**Figure 8a**).

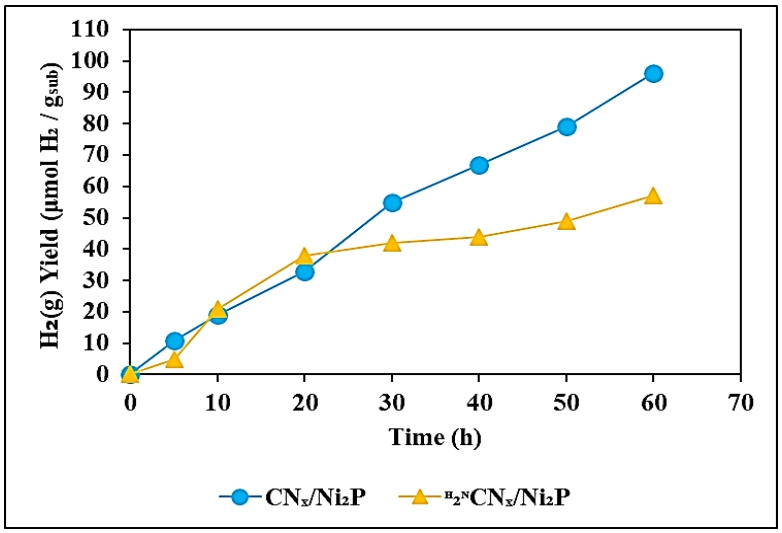

(a)

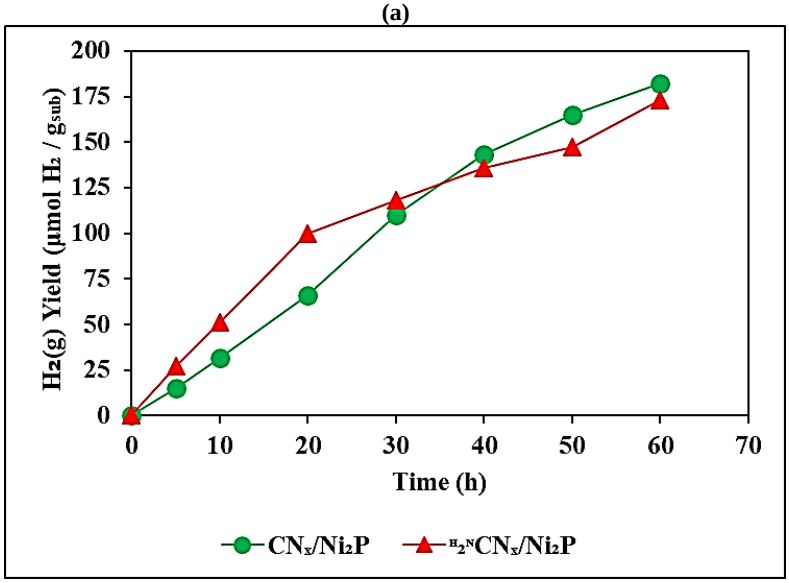

(b)

Figure 8: Comparison of photoreforming of **(a)** polyethylene terephthalate and **(b)** polylactic acid over CN_x/Ni_2P and $^{H2N}CN_x/Ni_2P$. Experimental conditions: at 4.8 mg/ml CN_x/Ni_2P photocatalyst, at pre-treated 20 mg/ml polyethylene terephthalate, at pre-treated 20 mg/ml polylactic acid, at 4 ml aqueous 1M KOH, at 10 ml internal volume of sealed photoreactor under anaerobic conditions, at 1200 W Xe solar lamp, at 60 h, at AM 1.0G, at 150 mW/cm^2, at 25°C, respectively.

15, 32, 66, 110, 143 and 165 µmol H_2 / g_{sub} H_2(g) yields for polylactic acid over CN_x/Ni_2P were observed after 5, 10, 20, 30, 40 and 50 h photoreforming solar irradiation times, respectively, at 4.8 mg/ml CN_x/Ni_2P photocatalyst, at pre-treated 20 mg/ml polylactic acid, at 4 ml aqueous 1 M KOH, at 10 ml internal volume of sealed photoreactor under anaerobic conditions, at 1200 W Xe solar lamp, at AM 1.0G, at 150 mW/cm^2, at 25°C, respectively (**Figure 8b**). The maximum 182 µmol H_2 / g_{sub} H_2(g) yields for polylactic acid over CN_x/Ni_2P were obtained after 60 h photoreforming solar irradiation time, at 4.8 mg/ml CN_x/Ni_2P photocatalyst, at pre-treated 20 mg/ml polylactic acid, at 4 ml aqueous 1 M KOH, at 10 ml internal volume of sealed photoreactor under anaerobic conditions, at 1200 W Xe solar lamp, at AM 1.0G, at 150 mW/cm^2, at 25°C, respectively (**Figure 8b**). 27, 51, 100, 118, 136 and 147 µmol H_2 / g_{sub} H_2(g) yields for polylactic acid over $^{H2N}CN_x/Ni_2P$ were measured after 5, 10, 20, 30,40 and 50 h photoreforming solar irradiation times, respectively, at 4.8 mg/ml CN_x/Ni_2P photocatalyst, at pre-treated 20 mg/ml polylactic acid, at 4 ml aqueous 1 M KOH, at 10 ml internal volume of sealed photoreactor under anaerobic conditions, at 1200 W Xe solar lamp, at AM 1.0G, at 150 mW/cm^2, at 25°C, respectively (**Figure 8b**). The maximum 173 µmol H_2 / g_{sub} H_2(g) yields for polylactic acid over $^{H2N}CN_x/Ni_2P$ were obtained after 60 h photoreforming solar irradiation time, at 4.8 mg/ml CN_x/Ni_2P photocatalyst, at pre-treated 20 mg/ml polylactic acid, at 4 ml aqueous 1 M KOH, at 10 ml internal volume of sealed photoreactor under anaerobic conditions, at 1200 W Xe solar lamp, at AM 1.0G, at 150 mW/cm^2, at 25°C, respectively (**Figure 8b**).

3. The By-Products Measurements of Polyethylene Terephthalate and Polylactic Acid

The GC-MS results was showed that both polyethylene terephthalate and polylactic acid form a variety of oxidation products after 12 h and 24 h photoreforming solar irradiation times, at 4.8 mg/ml CN_x/Ni_2P, at 20 mg/ml polyethylene terephthalate, at pre-treated 20 mg/ml polylactic acid, at 50 mg/ml polymer, at 4 ml aqueous 1 M KOH, at 10 ml internal volume of sealed photoreactor under anaerobic conditions, at 1200 W Xe solar lamp, at 24 h at AM 1.0G, at 150 mW/cm^2, at 25°C, respectively (**Table 5**).

Intermediates	Time (h)	Activity ($\mu mol\ H_2 / g_{cat}.h$)	H_2(g) Yield ($\mu mol\ H_2 / g_{sub}$)
Acetate	12	6.56 ± 0.84	1.68 ± 0.21
	24	3.77 ± 0.47	4.85 ± 0.62
Ethylene glycol	12	75.76 ± 3.75	19.35 ± 1.93
	24	69.15 ± 8.40	88.37 ± 10.74
Formate	12	25.20 ± 1.52	6.45 ± 0.70
	24	20.70 ± 1.16	26.55 ± 1.95
Glycolate	12	21.15 ± 1.32	5.37 ± 0.95
	24	17.42 ± 1.67	21.94 ± 1.86
Glyoxal	12	61.95 ± 3.15	15.90 ± 0.75
	24	58.82 ± 7.35	75.30 ± 9.34
Lactate	12	36.31± 4.60	9.30 ± 1.56
	24	47.43 ± 4.05	60.07 ± 5.11
Terephthalate	12	1.76 ± 0.15	3.58 ± 0.85
	24	6.20 ± 0.77	14.61 ± 2.14
Note: Yields and activities are cumulative values. The standard deviation (σ) calculated from 3 samples.			

Table 5: H_2(g) production during photoreforming of oxidation intermediates with CN_x/Ni_2P from GC-MS measurements results (Experimental conditions: at 4.8 mg/ml CN_x/Ni_2P, at pre-treated 20 mg/ml polyethylene terephthalate, at pre-treated 20 mg/ml polylactic acid, at 50 mg/ml polymer, at 4 ml aqueous 1M KOH, at 10 ml internal volume of sealed photoreactor under anaerobic conditions, at 1200 W Xe solar lamp, at 24 h at AM 1.0G, at 150 mW/cm^2, at 25°C, respectively).

The maximum 4.85 ± 0.62, 88.37 ± 10.74, 26.55 ± 1.95, 21.94 ± 1.86, 75.30 ± 9.34, 60.07 ± 5.11 and 14.61 ± 2.14 μmol H_2 / g_{sub} H_2(g) production yields were obtained for Acetate, Ethylene glycol, Formate, Glycolate, Glyoxal, Lactate and Terephthalate oxidation intermediates, respectively, after 24 h photoreforming solar irradiation times, at 4.8 mg/ml CN_x/Ni_2P, at 20 mg/ml polyethylene terephthalate, at pre-treated 20 mg/ml polylactic acid, at 50 mg/ml polymer, at 4 ml aqueous 1 M KOH, at 10 ml internal volume of sealed photoreactor under anaerobic conditions, at 1200 W Xe solar lamp, at 24 h at AM 1.0G, at 150 mW/cm^2, at 25°C, respectively (**Table 5**). The photoreforming process of lactic acid (the monomer of polylactic acid) is also faster on CN_x/Ni_2P (47.43 ± 4.05 μmol H_2 /g_{sub}. h, after 24 h photoreforming solar irradiation time at **Table 5**) than a reported H_2NCN_x/WS_2 system in H_2O (0.50 μmol H_2 /g_{sub}. h) (Hou et al., 2014). Quantification of organic oxidation intermediates for polyethylene terephthalate and polylactic acid with CN_x/Ni_2P after 7 days photoreforming process from ICP-MS measurements results were recorded at **Table 6**. 126 nmol Acetate, 131 nmol Formate, 5 nmol Glycolate and 6200 nmol Glyoxal organic oxidation intermediates for polyethylene terephthalate with CN_x/Ni_2P nanocatalyst were found after 7 days photoreforming solar irradiation time, at 4.8 mg/ml CN_x/Ni_2P, at 20 mg/ml polyethylene terephthalate, at 50 mg/ml polymer, at 4 ml aqueous 1 M KOH, at 10 ml internal volume of sealed photoreactor under anaerobic conditions, at 1200 W Xe solar lamp, at AM 1.0G, at 150 mW/cm^2, at 25°C, respectively (**Table 6).**

Parameters	Organic oxidation intermediates	Quantity (nmol)
Polyethylene terephthalate	Acetate	126
	Formate	131
	Glycolate	5
	Glyoxal	6200
Polylactic acid	Acetate	67
	Formate	63
Note 1: Yields and activities are cumulative values. The standard deviation (σ) calculated from 3 samples. **Note 2:** Reference standard: Maleic acid		

Table 6: Quantification of organic oxidation intermediates for polyethylene terephthalate and polylactic acid with CN_x/Ni_2P nanocatalyst after 7 days photoreforming process from ICP-MS measurements results (Experimental conditions: at 4.8 mg/ml CN_x/Ni_2P, at 20 mg/ml polyethylene terephthalate, at 50 mg/ml polymer, at 4 ml aqueous 1 M KOH, at 10 ml internal volume of sealed photoreactor under anaerobic conditions, at 1200 W Xe solar lamp, at AM 1.0G, at 150 mW/cm^2, at 25°C, respectively).

67 nmol Acetate and 63 nmol Formate organic oxidation intermediates for polylactic acid with CN_x/Ni_2P nanocatalyst were obtained after 7 days photoreforming solar irradiation time, at 4.8 mg/ml CN_x/Ni_2P, at pre-treated 20 mg/ml polylactic acid, at 50 mg/ml polymer, at 4 ml aqueous 1 M KOH, at 10 ml internal volume of sealed photoreactor under anaerobic conditions, at 1200 W Xe solar lamp, at AM 1.0G, at 150 mW/cm^2, at 25°C, respectively (**Table 6).**

3. Conclusions

The maximum 41.40 ± 5.10 and 48.60 ± 3.12 μmol H_2 / g_{sub} yields were measured for CN_x=20 mg/ml and for Ni_2P=20 mg/ml, respectively, with photoreforming process, at ultrasonicated 4.8 mg/ml CN_x/Ni_2P nanocatalyst, at pre-treated 20 mg/ml polyethylene terephthalate, at pre-treated 20 mg/ml polylactic acid, at 4 ml aqueous 1 M KOH, at 10 ml internal volume of sealed photoreactor under anaerobic conditions, at 1200 W Xe solar lamp, at 24 h, at AM 1.0G, at 150 mW/cm^2, at 25°C, respectively.

The maximum 18.26 ± 1.18 and 52..41 ± 7.29 μmol H_2 / g_{sub} H_2(g) production yields were found for non-sonicated CN_x/Ni_2P and ultra-sonicated CN_x/Ni_2P nanocatalyst, respectively, with photoreforming process, after 24 h photoreforming solar irradition time, at 4.8 mg/ml CN_x/Ni_2P, at 20 mg/ml polyethylene terephthalate, at pre-treated 20 mg/ml polylactic acid, at 4 ml aqueous 1 M KOH, at 10 ml internal volume of sealed photoreactor under anaerobic conditions, at 1200 W Xe solar lamp, at AM 1.0G, at 150 mW/cm^2, at 25°C, respectively. The maximum 123.75 ± 11.92 and 267.41 ± 24.65 μmol H_2 / g_{sub} H_2(g) production yield was measured for polyethylene terephthalate and

polylactic acid, respectively, with photoreforming process, after 60 h photoreforming solar irradiation time, at ultra-sonicated 4.8 mg/ml CN_x/Ni_2P, at pre-treated 50 mg/ml polymer, at 4 ml aqueous 1 M KOH, at 10 ml internal volume of sealed photoreactor under anaerobic conditions, at 1200 W Xe solar lamp, at AM 1.0G, at 150 mW/cm^2, at 25°C, respectively. The maximum 6.57 ± 0.87% and 2.43 ± 0.38% stoichiometric H_2 conversion yields were observed for polyethylene terephthalate and polylactic acid, respectively, with photoreforming process, after 60 h photoreforming solar irradition time, at 4.8 mg/ml CN_x/Ni_2P, at 20 mg/ml polyethylene terephthalate, at 20 mg/ml polylactic acid, at 50 mg/ml polymer, at 4 ml aqueous 1 M KOH, at 10 ml internal volume of sealed photoreactor under anaerobic conditions, at 1200 W Xe solar lamp, at AM 1.0G, at 150 mW/cm^2, at 25°C, respectively. The maximum 96 and 57 µmol H_2 / g_{sub} H_2(g) yields for polyethylene terephthalate were obtained over CN_x/Ni_2P and $^{H2N}CN_x/Ni_2P$, respectively, with photoreforming process, after 60 h photoreforming solar irradiation time, at 4.8 mg/ml CN_x/Ni_2P photocatalyst, at pre-treated 20 mg/ml polyethylene terephthalate, at 4 ml aqueous 1 M KOH, at 1200 W Xe solar lamp, at AM 1.0G, at 150 mW/cm^2, at 25°C, respectively. The maximum 182 and 173 µmol H_2 / g_{sub} H_2(g) yields for polylactic acid were observed over CN_x/Ni_2P and $^{H2N}CN_x/Ni_2P$, respectively, with photoreforming process, after 60 h photoreforming solar irradiation time, at 4.8 mg/ml CN_x/Ni_2P photocatalyst, at pre-treated 20 mg/ml polylactic acid, at 4 ml aqueous 1 M KOH, at 1200 W Xe solar lamp, at AM 1.0G, at 150 mW/cm^2, at 25°C, respectively. The maximum 4.85 ± 0.62, 88.37 ± 10.74, 26.55 ± 1.95, 21.94 ± 1.86, 75.30 ± 9.34, 60.07 ± 5.11 and 14.61 ± 2.14 µmol H_2 / g_{sub} H_2(g) production yields were obtained for Acetate, Ethylene glycol, Formate, Glycolate, Glyoxal, Lactate and Terephthalate oxidation intermediates, respectively, with photoreforming process, after 24 h photoreforming solar irradiation times, at 4.8 mg/ml CN_x/Ni_2P, at 20 mg/ml polyethylene terephthalate, at pre-treated 20 mg/ml polylactic acid, at 50 mg/ml polymer, at 4 ml aqueous 1 M KOH, at 10 ml internal volume of sealed photoreactor under anaerobic conditions, at 1200 W Xe solar lamp, at AM 1.0G, at 150 mW/cm^2, at 25°C, respectively. 126 nmol Acetate, 131 nmol Formate, 5 nmol Glycolate and 6200 nmol Glyoxal organic oxidation intermediates for polyethylene terephthalate with CN_x/Ni_2P nanocatalyst were found with photoreforming process, after 7 days photoreforming solar irradiation time, at 4.8 mg/ml CN_x/Ni_2P, at 20 mg/ml polyethylene terephthalate, at 50 mg/ml polymer, at 4 ml aqueous 1 M KOH, at 10 ml internal volume of sealed photoreactor under anaerobic conditions, at 1200 W Xe solar lamp, at AM 1.0G, at 150 mW/cm^2, at 25°C, respectively. 67 nmol Acetate and 63 nmol Formate organic oxidation intermediates for polylactic acid with CN_x/Ni_2P nanocatalyst were observed with photoreforming process, after 7 days photoreforming solar irradiation time, at 4.8 mg/ml CN_x/Ni_2P, at pre-treated 20 mg/ml polylactic acid, at 50 mg/ml polymer, at 4 ml aqueous 1 M KOH, at 10 ml internal volume of sealed photoreactor under anaerobic conditions, at 1200 W Xe solar lamp, at AM 1.0G, at 150 mW/cm^2, at 25°C, respectively. High H_2(g) production efficiency was obtained by photoreforming process for the production of H_2(g) from real polyethylene terephthalate and polylactic acid wastes using CN_x/Ni_2P nanocatalyst. Photoreforming process is a very effective, easy to apply, economical and environmentally friendly method for the removal of plastic and microplastic wastes.

Acknowledgement: This research study was undertaken in the Environmental Microbiology Laboratories at Dokuz Eylül University Engineering Faculty Environmental Engineering Department, Izmir, Turkey. The authors would like to thank this body for providing financial support.

References

1. Andrady, A.L. (2015). Persistence of plastic litter in the oceans. In Marine Anthropogenic Litter; Springer International Publishing: Cham, 57−72.
2. Cao, S., Low, J., Yu, J., Jaroniec, M. (2015). Polymeric photocatalysts based on graphitic carbon nitride. Adv. Mater., 27:2150–2176.
3. Cao, S., Wang, C.-J., Fu, W.-F., Chen, Y. (2017). Metal phosphides as co-catalysts for photocatalytic and photoelectrocatalytic water splitting. Chem Sus Chem, 10:4306−4323.
4. Caputo, C.A., Gross, M.A., Lau, V.W.-H., Cavazza, C., Lotsch, B.V., et al. (2014). Photocatalytic hydrogen production using polymeric carbon nitride with a hydrogenase and a bioinspired synthetic Ni catalyst. Angew. Chemie Int. Ed., 53:11538–11542.
5. Chen, W.-T., Jin, K., Linda Wang, N.-H. (2019). Use of supercritical water for the liquefaction of polypropylene into oil. ACS Sustainable Chem. Eng., 7:3749−3758.
6. Cozar, A., Echevarría, F., Gonza´lez-Gordillo, J.I., Irigoien, X.,´ Ú beda, B., et al. (2014). Plastic´ debris in the open ocean. Proc. Natl. Acad. Sci. U.S.A., 111:10239−10244.
7. Creissen, C.E., Warnan, J., Reisner, E. (2018). Solar H_2 generation in water with a $CuCrO_2$ photocathode modified with an organic dye and molecular Ni catalyst. Chem. Sci., 9:1439–1447.
8. Cui, Y., Ding, Z., Liu, P., Antonietti, M., Fu, X., et al. (2012). Metal-free activation of H_2O_2 by g-C_3N_4 under visible light irradiation for the degradation of organic pollutants. Phys. Chem. Chem. Phys., 14:1455–1462.
9. Ding, Z., Chen, X., Antonietti, M., Wang, X. (2011). Synthesis of transition metal modified carbon nitride polymers for selective hydrocarbon oxidation. ChemSusChem, 4:274–281.
10. Ellen MacArthur Foundation. (2017a). The New Plastics Economy: Rethinking the Future of Plastics & Catalysing Action.
11. Emel'yanenko, V.N., Verevkin, S.P., Schick, C., Stepurko, E.N., Roganov, G.N., et al. (2010). The thermodynamic properties of S-Lactic acid. Russ. J. Phys. Chem. A, 84:1491–1497.
12. Gao, L.-F., Wen, T., Xu, J.-Y., Zhai, X.-P., Zhao, M., et al. (2016). Iron-doped carbon nitride-type polymers as homogeneous organocatalysts for visible light-driven hydrogen evolution. ACS Appl. Mater. Interfaces, 8:617–624.
13. Garcia, J.M., Robertson, M.L. (2017). The future of plastics recycling. Science, 358:870−872.
14. Geyer, R., Jambeck, J.R., Law, K.L. (2017). Production, use, and fate of all plastics ever made. Sci. Adv., 3: No. e1700782.
15. Gong, Y., Li, M., Wang, Y. (2015). Carbon nitride in energy conversion and storage: recent advances and future prospects. ChemSusChem, 8:931–946.
16. Gross, M.A., Reynal, A., Durrant, J.R., Reisner, E. (2014). Versatile photocatalytic systems for H_2 generation in water based on an efficient dubois-type nickel catalyst. J. Am. Chem. Soc., 136:356–366.
17. Helm, M.L., Stewart, M.P., Bullock, R.M., DuBois, M.R., DuBois, D.L., (2011). A synthetic nickel electrocatalyst with a turnover frequency above 100,000 s-1 for H_2 production. Science, 333:863–866.
18. Horikoshi, S., Serpone, N., Hisamatsu, Y., Hidaka, H. (1998). Photocatalyzed degradation of polymers in aqueous semiconductor suspensions. 3. photooxidation of a solid polymer: TiO_2-blended poly (vinyl chloride) film. Environ. Sci. Technol., 32:4010− 4016.

19. Hou, Y., Zhu, Y., Xu, Y., Wang, X. (2014). Photocatalytic hydrogen production over carbon nitride loaded with WS_2 as cocatalyst under visible light. Appl. Catal., B, 156−157:122−127.
20. Indra, A., Acharjya, A., Menezes, P.W., Merschjann, C., Hollmann, D., et al. (2017).Boosting visible-light-driven photocatalytic hydrogen evolution with an integrated nickel phosphide carbon nitride system. Angew. Chem., Int. Ed., 56:1653−1657.
21. International Energy Agency (IEA). (2015). Tracking Clean Energy Progress 2015: Energy Technology Perspectives 2015 Excerpt IEA Input to the Clean Energy Ministerial; Paris.
22. Kasap, H., Achilleos, D.S., Huang, A., Reisner, E. (2018). Photoreforming of lignocellulose into H_2 using nanoengineered carbon nitride under benign conditions. J. Am. Chem. Soc., 140:11604−11607.
23. Kasap, H., Caputo, C.A., Martindale, B.C.M., Godin, R., Lau, V.W.-H., (2016). Solar-driven reduction of aqueous protons coupled to selective alcohol oxidation with a carbon nitride–molecular in catalyst system. J. Am. Chem. Soc., 138:9183–9192.
24. Kawai, T., Sakata, T. (1981). Photocatalytic hydrogen production from water by the decomposition of poly-vinylchloride, protein, algae, dead insects, and excrement. Chem. Lett., 10:81−84.
25. Kilgore, U.J., Roberts, J.A.S., Pool, D.H., Appel, A.M., Stewart, M.P., et al. (2011). $[Ni(PPh_2NC_6H_4X)_2]^{2+}$ Complexes as electrocatalysts for H_2 production: effect of substituents, acids, and water on catalytic rates. J. Am. Chem. Soc., 133:5861–5872.
26. Kosuth, M., Mason, S.A., Wattenberg, E.V. (2018). Anthropogenic contamination of tap water, beer, and sea salt. PLoS One, 13: No. e0194970.
27. Kuehnel, M.F., Reisner, E. (2018). Solar hydrogen generation from lignocellulose. Angew. Chem., Int. Ed., 57:3290−3296.
28. Lau, V.W.-H., Moudrakovski, I., Botari, T., Weinberger, S., Mesch, M.B., et al. (2016). Rational design of carbon nitride photocatalysts by identification of cyanamide defects as catalytically relevant sites. Nat. Commun., 7:12165.
29. Law, K.L., Thompson, R.C. (2014). Microplastics in the Seas. Science, 345:144−145.
30. Leung, J.J., Warnan, J., Nam, D.H., Zhang, J.Z., Willkomm, J., et al. (2017). Photoelectrocatalytic H_2 evolution in water with molecular catalysts immobilised on p-Si via a stabilising mesoporous TiO_2 interlayer. Chem. Sci., 8:5172–5180.
31. Li, J., Shen, B., Hong, Z., Lin, B., Gao, B., et al. (2012). A facile approach to synthesize novel oxygen-doped g-C_3N_4 with superior visible-light photoreactivity. Chem. Commun., 48:12017–12019.
32. Li, Z., Kong, C., Lu, G. (2016). Visible photocatalytic water splitting and photocatalytic two-electron oxygen formation over Cu- and Fe-doped g-C_3N_4. J. Phys. Chem. C, 120:56–63.
33. Lin, L., Yu, Z., Wang, X. (2019). Crystalline carbon nitride semiconductors for photocatalytic water splitting. Angew. Chem., Int. Ed., 58:6164−6175.
34. Liu, J., Liu, Y., Liu, N., Han, Y., Zhang, X., et al. (2015). Metal-free efficient photocatalyst for stable visible water splitting via a two-electron pathway. Science, 347:970–974.
35. MacArthur, E. (2017b). Beyond plastic waste. Science, 358:843.
36. Maeda, K., Wang, X., Nishihara, Y., Lu, D., Antonietti, M., et al. (2009). Photocatalytic activities of graphitic carbon nitride powder for water reduction and oxidation under visible light. J. Phys. Chem. C, 113:4940–4947.
37. Mason, S.A., Welch, V.G., Neratko, J. (2018). Synthetic polymer contamination in bottled water. Front. Chem., 6:407.
38. Meyer, A.U., Lau, V.W., König, B., Lotsch, B.V. (2017). Photocatalytic oxidation of sulfinates to vinyl sulfones with cyanamide-functionalised carbon nitride. Eur. J. Org. Chem., 2179−2185.
39. NIST Chemistry WebBook. 1,2-Ethanediol https://webbook.nist.gov/cgi/cbook.cgi?ID=C107211&Mask=2 (accessed July 16, 2023).
40. Ohtani, B., Adzuma, S., Nishimoto, S., Kagiya, T. (1992). Photocatalytic degradation of polyethylene film by incorporated extra fine particles of titanium dioxide. Polym. Degrad. Stab., 35:53−60.
41. Pellegrin, Y., Odobel, F. (2017). Sacrificial electron donor reagents for solar fuel production. C.R. Chim., 20:283−295.
42. Pivokonsky, M., Cermakova, L., Novotna, K., Peer, P., Cajthaml, T., et al. (2018). Occurrence of microplastics in raw and treated drinking Water. Sci. Total Environ., 643:1644−1651.
43. Puga, A.V. (2016). Photocatalytic production of hydrogen from biomass-derived feedstocks. Coord. Chem. Rev., 315:1−66.
44. Qiu, P., Chen, H., Xu, C., Zhou, N., Jiang, F., et al. (2015). Fabrication of an exfoliated graphitic carbon nitride as a highly active visible light photocatalyst. J. Mater. Chem. A, 3:24237–24244.
45. Spath, P.L., Mann, M.K. (2001). Life Cycle Assessment of Hydrogen Production via Natural Gas Steam Reforming; Golden.
46. Su, F., Mathew, S.C., Lipner, G., Fu, X., Antonietti, M., et al. (2010). mpg-C_3N_4-catalyzed selective oxidation of alcohols using O_2 and visible light. J. Am. Chem. Soc., 132:16299–16301.
47. The United States Department of Energy (DOE). (2013). Report of the Hydrogen Production Expert Panel: A Subcommittee of the Hydrogen & Fuel Cell Technical Advisory Committee; Washington DC, USA.
48. Thomas, A., Fischer, A., Goettmann, F., Antonietti, M., Müller, J.-O., et al. (2008). Graphitic carbon nitride materials: variation of structure and morphology and their use as metal-free catalysts. J. Mater. Chem., 18:4893−4908.
49. Tofa, T.S., Kunjali, K.L., Paul, S., Dutta, J. (2019). Visible light photocatalytic degradation of microplastic residues with zinc oxide nanorods. Environ. Chem. Lett., 17:1341−1346.
50. Uekert, T., Kuehnel, M.F., Wakerley, D.W., Reisner, E. (2018). Plastic waste as a feedstock for solar-driven H_2 generation. Energy Environ. Sci., 11:2853−2857.
51. Vilela, F., Zhang, K., Antonietti, M. (2012). Conjugated porous polymers for energy applications. Energy Environ. Sci., 5:7819–7832.
52. Wakerley, D.W., Kuehnel, M.F., Orchard, K.L., Ly, K.H., Rosser, T.E., et al. (2017). Solar-driven reforming of lignocellulose to H_2 with a CdS/CdO_x photocatalyst. Nat. Energy, 2:17021.
53. Wang, X., Maeda, K., Thomas, A., Takanabe, K., Xin, G., et al. (2009). A metal-free polymeric photocatalyst for hydrogen production from water under visible light. Nat. Mater., 8:76–80.
54. Wang, Y., Li, H., Yao, J., Wang, X., Antonietti, M. (2011). Synthesis of boron doped polymeric carbon nitride solids and their use as metal-free catalysts for aliphatic C–H bond oxidation. Chem. Sci., 2:446–450.
55. Wen, J., Xie, J., Shen, R., Li, X., Luo, X., et al. (2017). Markedly enhanced visible-light photocatalytic H_2 generation over g-C_3N_4 nanosheets decorated by robust nickel phosphide ($Ni_{12}P_5$) cocatalysts. Dalt. Trans., 46:1794−1802.

56. Yang, S., Gong, Y., Zhang, J., Zhan, L., Ma, L., et al. (2013). Exfoliated graphitic carbon nitride nanosheets as efficient catalysts for hydrogen evolution under visible light. Adv. Mater., 25:2452–2456.
57. Ye, P., Liu, X., Iocozzia, J., Yuan, Y., Gu, L., et al. (2017). A highly stable non-noble metal Ni_2P co-catalyst for increased H_2 generation by g-C_3N_4 under visible light irradiation. J. Mater. Chem. A, 5:8493−8498.
58. Zhan, Y., Liu, Z., Liu, Q., Huang, D., Wei, Y., et al. (2017). A facile and one-pot synthesis of fluorescent graphitic carbon nitride quantum dots for bio-imaging applications. New J. Chem., 41:3930–3938.
59. Zhang, Y., Mori, T., Ye, J., Antonietti, M. (2010). Phosphorus-doped carbon nitride solid: Enhanced electrical conductivity and photocurrent generation. J. Am. Chem. Soc., 132:6294–6295.
60. Zhu, M., Kim, S., Mao, L., Fujitsuka, M., Zhang, J., et al. (2017). Metal-free photocatalyst for H_2 evolution in visible to near-ınfrared region: black phosphorus/graphitic carbon nitride. J. Am. Chem. Soc., 139:13234–13242.

DOI:10.31579/2690-4861/332